processes

MDPI

Article

# Process of Obtaining Chromium Nitride in the Combustion Mode under Conditions of Co-Flow Filtration

**Nikolay Evseev [1,2,*], Mansur Ziatdinov [2], Vladimir Romandin [2], Alexander Zhukov [2], Aidos Tolynbekov [2] and Yuliya Ryzhikh [2]**

[1] Institute for Problems of Chemical and Energetic Technologies of the Siberian Branch of the Russian Academy of Sciences, 659322 Biysk, Russia

[2] Laboratory of High-Energy Systems and New Technologies, National Research Tomsk State University, 634050 Tomsk, Russia; ziatdinovm@mail.ru (M.Z.); romandin@niipmm.tsu.ru (V.R.); zhuk_77@mail.ru (A.Z.); tolynbekov_aidos@mail.ru (A.T.); jula@ftf.tsu.ru (Y.R.)

* Correspondence: evseevns@gmail.com

Received: 10 July 2020; Accepted: 28 August 2020; Published: 30 August 2020




**Abstract:** In this work, the combustion process of chromium powder in the co-flow filtration mode was studied. The effect of nitrogen-containing gas flow rate on the nitridation of combustion products is shown. The effect of the amount of argon in the nitrogen–argon mixture on the burning rate and the burning temperature of the chromium powder is shown. It was found that an increase in the percentage of argon in the nitrogen–argon mixture can lead to the formation of an inverse combustion wave. The actual burning temperature is higher than adiabatic burning temperature in the co-flow filtration mode, thus the phenomenon of superadiabatic heating is observed. The phase composition of the obtained combustion products was studied. It was shown that the forced filtration mode allows for synthesizing non-stoichiometric $Cr_2N$ nitride.

**Keywords:** filtration combustion; co-flow; self-propagating high-temperature synthesis; superadiabatic heating; nitrogen–argon mixture; inverse combustion wave; chromium nitride

## 1. Introduction

The development of modern technology is impossible without the creation of new materials. The widespread use of metal nitrides is due to their physical and chemical properties, such as heat resistance, corrosion resistance, and wear resistance. Metal nitrides are used as abrasive materials, and wear-resistant and decorative coatings. The most important possible areas of the practical application of metal nitrides are their use as master alloys to increase the heat resistance of metal materials, initial powders for nitride ceramics, and as master alloys to increase the cold resistance of steel. Thus, obtaining metal nitrides and studying their properties is a critical task.

To date, the industry uses well-known methods of powder metallurgy to produce metal nitrides. The most common are the furnace method, plasma chemical synthesis, and self-propagating high temperature synthesis (SHS). The main disadvantages of the furnace method and plasma chemical synthesis are high energy costs and expensive equipment. The SHS method allows for achieving high performance at low energy costs; however, it requires the use of high-pressure reactors.

The traditional SHS of nitrides and filtration combustion of metal powders in nitrogen are experimentally studied under conditions of natural filtration in high pressure reactors, where, due to the pressure drop, the reaction gas is supplied to the combustion region [1–10]. There is a different type of filtration combustion in which the reacting gas is forced into the combustion zone and moves in the direction of combustion through the reaction products [11].

This type of combustion is theoretically described in sufficient detail [12–17], but at the same time, it has been little studied experimentally [18–20]. Most of these works deal with the study of combustion of a mixture of titanium and carbon powders in a co-flow of nitrogen and/or argon. The combustion of a granular mixture of titanium and carbon was studied in [21,22]. The combustion of carbon-containing fuel in a stream of oxygen-containing gas was studied in [23–25]. The mechanism and combustion regularities of chromium in nitrogen under conditions of natural filtration were studied in [26,27].

The study of chromium combustion in this paper is justified by its high melting point (~1900 °C) with a relatively low exothermicity ($Cr_2N$ $T_{ad}$ = 1287 °C; CrN $T_{ad}$ = 2050 °C, where $T_{ad}$ is the calculated adiabatic temperature). This allows to exclude the influence of melting of the initial powder and synthesis products on the filtration process.

The process of chromium combustion in the mode of co-flow filtration is considered in this paper. This method is energy efficient and has a high application value. Natural filtering mode is self-regulatory—i.e., processes in the combustion zone determine the interaction of the burning sample with the environment. With forced filtration, this interaction is initially set and defined by the characteristics of the gas flow. The implementation of the combustion of metal powders in a co-flow of nitrogen-containing gas can bring quality changes to the process.

The aim of this work is to experimentally study the combustion of chromium powder under forced filtration conditions and to study the properties of SHS products obtained as a result of combustion of chromium in a co-flow of nitrogen-containing gas.

## 2. Materials and Methods

As an initial material, chromium powder PH1S (Technical Specifications TU 14-1-1474-75) with a chromium content of 99.5% and a particles size less than 80 μm was used.

The particle size distribution of the initial powders was determined using an ANALYSETTE 22 MicroTec plus device from FRITSCH by laser diffraction. The nitrogen content was determined using a TCH600 device from LECO. The phase composition of specimens was obtained using a Rigaku diffractometer with CuKα radiation, as well as the Crystallographica Search Match program (Oxford Cryosystems—UK) based on the Powder Diffraction File database (PDF 4+). A Philips SEM 515 scanning electron microscope (SEM, Amsterdam, The Netherlands) was used to investigate the structure of the SHS products.

Experiments have shown that powder in the initial state has low porosity, which complicates the combustion process. The powder layer, consisting of such a powder, has a porosity of 64%. When gas was supplied, such a powder was compacted and hindered the filtration process. To increase the porosity of the samples, two approaches were used in this work. The essence of the first is the removal of a fine fraction and the production of a powder with a particle size of δ = 63–80 μm. In another case, the starting chromium powder (−80 μm) was granulated using polyvinyl alcohol. For the experiments, granules with a size of 500–1000 μm were used. The porosity of the sifted powder was 78%, and the granular powder was 72%.

The granulation process of chromium powder was carried out as follows. The chromium powder was mixed with a 3% solution of polyvinyl alcohol, until a consistency in which a homogeneous plastic mass was formed. Then, the obtained mixture was sieved (sieve classification of ~ 18 mesh) and sintered in a vacuum furnace at a temperature of 1100 °C. The holding time was 1 h. The obtained product was subsequently sieved twice (sieve classification of ~ 18 mesh and ~ 32 mesh). Thus, the granules were obtained, the sizes of which were in the range of 500–1000 μm.

The process of filtration combustion under forced filtration was carried out on the original equipment—laboratory SHS reactor—the scheme of which is shown in Figure 1. The laboratory co-flow reactor is made of complex devices consisting of a reactor (a), a gas supply unit (b) and a unit for registering and processing data (c). In Figure 1, the symbols G, P, T indicate the possibility of registering gas flow rate, pressure and temperature.

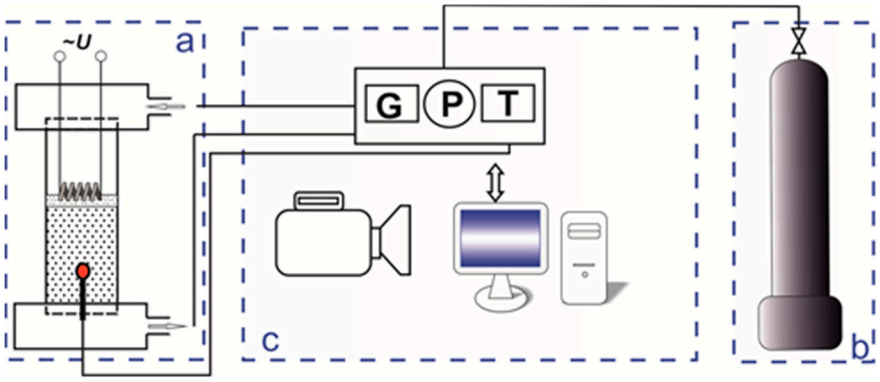



**Figure 1.** Scheme of an experimental equipment for studying combustion metals under forced filtration. (a) a reactor; (b) a gas supply unit; (c) a unit for registering and processing data.

Preparation of the experiments included the following steps. The initial powder was placed in a quartz tube. The size of the layer was constant: diameter 16 mm, height 50 mm. The upper part of the powder was brought into contact with an electric spiral. The quartz tube was sealed. The lower part of the quartz tube was pre-filled with a layer of aluminum oxide powder, which served to cool the gases. Using a reducer, the reaction gas was fed into the quartz tube from a gas cylinder containing a mixture of gases of a given composition.

An exothermic reaction was initiated by applying an electric pulse to the molybdenum helix in the surface layer. Burning front was formed, which began to spread along the sample. The gas flow rate was regulated by a reducer. Pressure monitoring was performed according to the readings of the pressure gauge and pressure sensor. Gas flow at the reactor inlet and outlet was carried out by electronic micro flowmeters of the thermo-anemometric type. The reaction temperature was measured by a W/Re thermocouple WR5/20, whose signal was transmitted through an amplifier to the recording device. The cooling chamber was used to cool the gaseous reaction products before entering the electronic flow meter. Process parameters were recorded by a multi-channel meter with processing and archiving on a computer.

The original co-flow SHS reactor allowed us to explore the combustion of metals in the nitrogen-containing gas in the co-flow filtration mode.

## 3. Results

### *3.1. Chromium Combustion in a Nitrogen Coflow*

The initiation of the combustion of chromium powder was carried out by applying a current to the molybdenum spiral, which resulted in the formation of a burning front that propagated along the sample. Figure 2 shows a typical photographic record of the propagation of the burning front in the co-flow filtration mode.

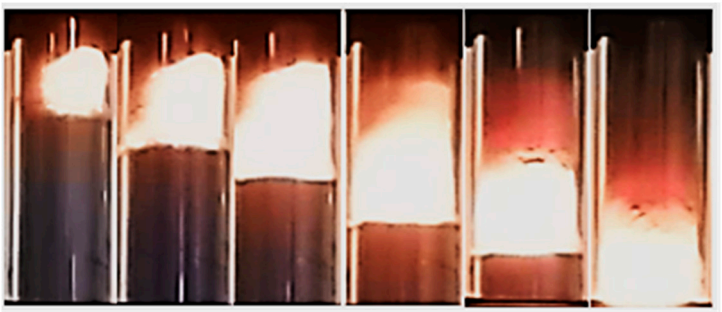


**Figure 2.** Propagation of the burning front during combustion of chromium powder in the co-flow filtration mode.

Until the electric current is supplied to the initiating helix, the readings of the flow meters at the input and output are the same. This is due to the fact that there is no absorption of the gas component by the dispersed medium located in the reactor. The absorption of the reacting component of the gas mixture begins after the reaction is initiated. In this case, the gas flow rate at the outlet of the reactor decreases, which is confirmed by the flow meter at the outlet of the reactor.

Table 1 shows the speed and maximum burning temperature of the powder and granules of chromium with a specific nitrogen flow rate of 12 $cm^3/(s \cdot cm^2)$.

**Table 1.** Maximum temperature and burning rate of chromium in nitrogen.

| | δ, μm | |
|---|---|---|
| | 63–80 | 500–1000 |
| u, mm/s | 2.4 | 0.82 |
| $T_{max}$, °C | 1640 | 1488 |
| [N], % | 7.5 | 7.8 |

According to Table 1, the chromium powder has a higher burning rate and burning temperature than of chromium granules.

Figure 3 presents the dependence of the nitridation of chromium on the nitrogen flow rate. The figure shows that when nitrogen flow rate ($q$) increases, the degree nitridation (η) decreases, and the maximum degree of nitriding is not achieved.

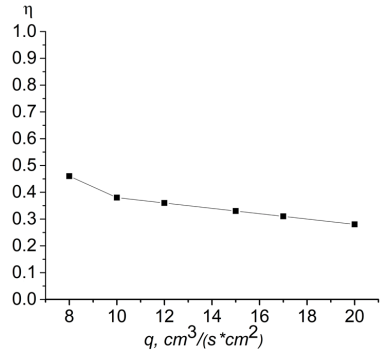



**Figure 3.** The effect of nitrogen flow rate on the nitridation of powder of chromium. $[N_2]$ = 100%.

Figure 4 shows the temperature profiles obtained by the combustion of powder (1) and granules (2) of chromium at a specific nitrogen flow rate of 12 $cm^3/(s \cdot cm^2)$. It can be seen from the figure that, when the chromium powder is burned, the heating zone is small and the burning temperature increases more rapidly.

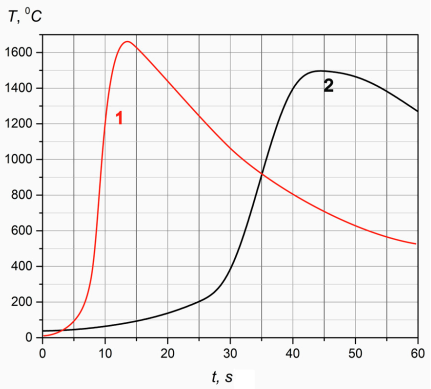



**Figure 4.** The temperature profiles obtained by combustion of powder (1) and granules (2) of chromium: $q$ = 12 $cm^3/(s \cdot cm^2)$; $[N_2]$ = 100%.

### *3.2. Chromium Combustion in a Co-Flow Nitrogen-Argon Mixture*

The addition of inert argon can significantly affect the combustion process. The greater the amount of cold ballast gas (argon) that enters the reaction zone, the more energy will be spent on heating it and the more heat will be redistributed.

#### 3.2.1. The Effect of the Amount of Argon in a Nitrogen-Argon Mixture on the Burning Speed and Burning Temperature of Chromium

The amount of argon in the nitrogen–argon mixture has the strongest effect not only on the rate and burning temperature of chromium, but also on the structure of the combustion wave, which appears in the form of temperature profiles. In Table 2, we gathered the burning rates and maximum burning temperatures of chromium at different argon contents in the nitrogen–argon mixture at a specific flow rate of 12 $cm^3/(s \cdot cm^2)$. According to Table 2, with an increase in the argon content (% mass), the temperature and the burning rate decrease significantly. It is also seen that granular chromium has lower burning rates and temperatures compared to chromium powder.

**Table 2.** Maximum temperature and burning rate of chromium, depending on the content of argon.

| | **$N_2$** | | **$N_2$+7% Ar** | | **$N_2$+12.8% Ar** | | **$N_2$+24% Ar** | |
|---|---|---|---|---|---|---|---|---|
| δ, μm | 63–80 | 500–1000 | 63–80 | 500–1000 | 63–80 | 500–1000 | 63–80 | 500–1000 |
| u, mm/s | 2.4 | 0.82 | 1.3 | – | 1.2 | 0.77 | 0.67 | 0.53 |
| $T_{max}$, °C | 1640 | 1488 | 1440 | – | 1460 | 1478 | 1240 | 1143 |

Figure 5 presents the temperature profiles obtained at the combustion of chromium granules at a specific flow rate of 12 $cm^3/(s \cdot cm^2)$, depending on the amount of argon in the nitrogen–argon mixture.

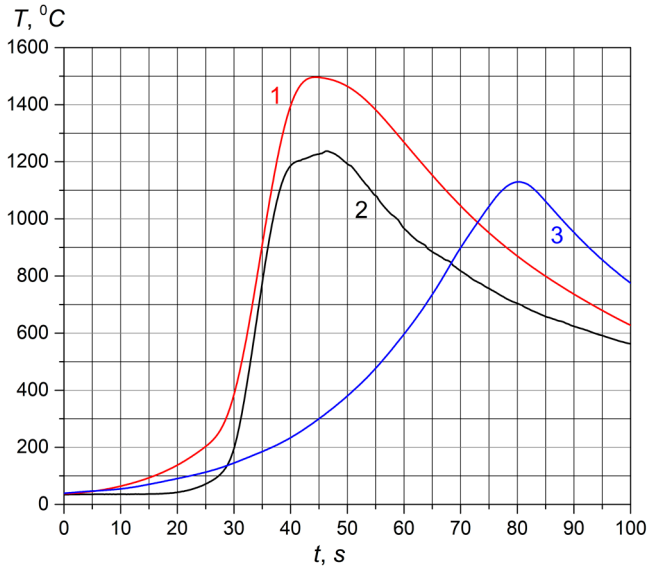



**Figure 5.** Temperature profiles at different argon content: $q$ = 12 $cm^3/(s \cdot cm^2)$; 1—[$N_2$] = 100%; 2—[Ar] = 12.8%; 3—[Ar] = 24%.

It was found that the composition of the gas mixture has a significant effect on the combustion process, and the temperature profiles have a qualitative difference.

The temperature profile is deformed, as follows. At combustion in nitrogen co-flow, the temperature profile has a small heating zone and a rapid increase in temperature to a maximum value. The maximum temperature zone has a small flat area. At [Ar] = 12.8%, the temperature profile also has a small heating zone; however, there is a long horizontal section with a maximum temperature.

There is a long cooling zone. When increasing argon to 24%, the temperature profile has a wide heating zone and a narrow section with a maximum temperature.

#### 3.2.2. The Effect of Flow Rate of Nitrogen–Argon Mixture on the Nitridation of Chromium

Table 3 shows the effect of the flow rate of gas mixture with 12.8% [Ar] on the nitridation of chromium. According to Table 3, the nitridation of chromium decreases slightly when increasing the flow rate of the nitrogen–argon mixture.

**Table 3.** Effect of flow rate of nitrogen–argon mixture on the nitridation of chromium.

| Initial Powder Size δ, μm | $q$ = 12 cm$^3$/(s·cm$^2$) | $q$ = 40 cm$^3$/(s·cm$^2$) |
|---|---|---|
| 63–80 | 8.4% | 8.0% |
| 500–1000 | 9.5% | 8.7% |

### *3.3. Phase Composition of Combustion Products*

A typical XRD patterns of combustion products at the combustion of powder (Figure 6a) and granules (Figure 6b) of chromium in the co-flow filtration mode at a gas flow rate of 12 cm$^3$/(s·cm$^2$), [Ar] = 12.8%, are presented in Figure 6. In both cases, $Cr_2N$ nitride and chromium were detected. XRD patterns in both cases are almost the same. XRD-analysis showed that the unit cell of the obtained $Cr_2N$ samples has trigonal lattice parameters.

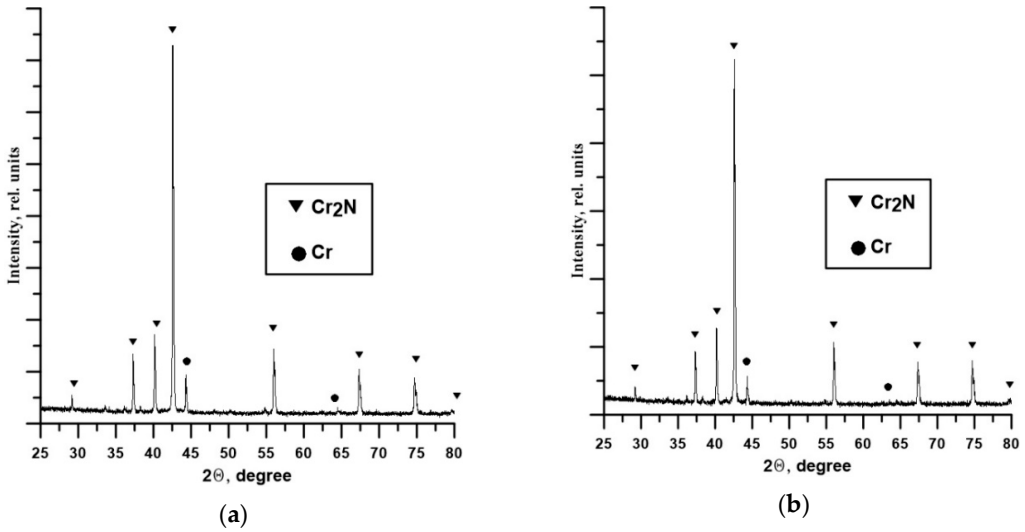



**Figure 6.** XRD patterns of samples obtained as a result of combustion of chromium in a flow reactor: (**a**)—for powder; (**b**)—for granules; $q$ = 12 cm$^3$/(s·cm$^2$); [Ar] = 12.8%.

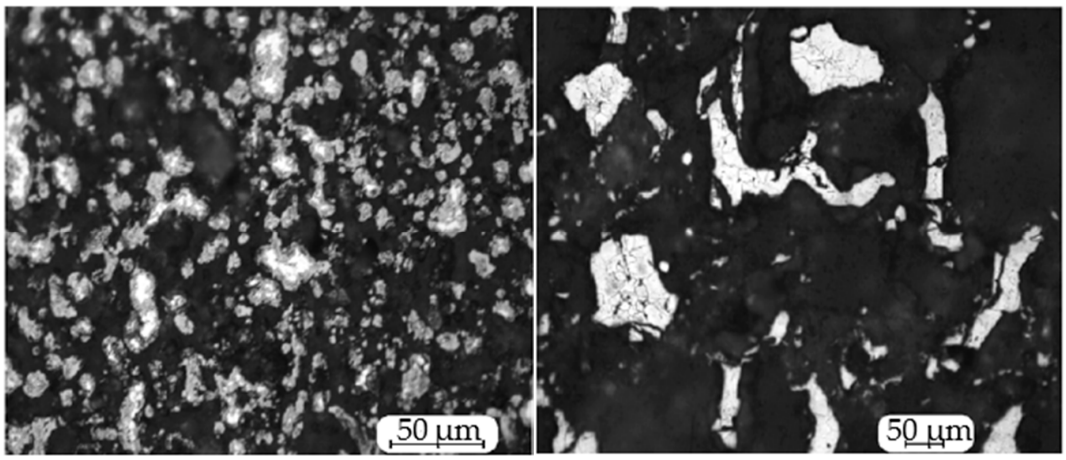
The photographs of synthesized $Cr_2N$ samples are presented in Figure 7. A sample of $Cr_2N$, obtained by the combustion of chromium powder, is shown in Figure 7a. A sample of $Cr_2N$ obtained by the combustion of granules of chromium is shown in Figure 7b,c. It has been established that, in the case of the combustion of chromium powder, and in the case of the combustion of granular chromium, the combustion products retain their initial structure. Synthesized $Cr_2N$ samples are easily destructible gray sinter. Milling the combustion products results in particles of the initial size.



(**a**) (**b**) (**c**)

**Figure 7.** Photographs of synthesized $Cr_2N$ samples. (**a**) obtained by the combustion of chromium powder; (**b**,**c**) obtained by the combustion of granules of chromium.

The microstructure of a $Cr_2N$ sample, obtained by the combustion of chromium powder in a co-flow of nitrogen–argon mixture ($q$ = 12 $cm^3/(s \cdot cm^2)$; [Ar] = 7%), in comparison with the microstructure of a $Cr_2N$ powder obtained under natural filtration mode at p = 0.2 MPa (the method is described in [26]), is presented in Figure 8.




(**a**) (**b**)

**Figure 8.** Microstructure of chromium sample at combustion in natural (**a**) and forced (**b**) filtration mode.

## 4. Discussion

1. To achieve a stable propagation of the combustion wave using chromium powder with a particle size δ = 63–80 μm when purged with pure nitrogen, it is necessary that the specific flow rate is more than 8 $cm^3/(s \cdot cm^2)$. A further decrease in specific consumption leads to a lack of fuel and a breakdown of combustion. The upper limit of the specific flow rate, when using pure nitrogen, is 20 $cm^3/(s \cdot cm^2)$. The reason for this is the rapid increase in the burning temperature with the eutectic melting point Cr–$Cr_2N$ reached. The appearance of the liquid phase violently changes the filtration conditions and leads to either non-stationary combustion, or to extinction.
2. Burning temperature decrease (Table 2), with an increase in the argon content in the mixture, is obviously related to the following fact. The reaction zone receives a large amount of cold gas ballast (argon), and a larger share of energy is spent on heating it. Further increase in the share of argon (more than 24%) in the nitrogen-containing gas leads to a breakdown of combustion and the impossibility of further propagation of the front. Reducing burning temperature by increasing the size of the particles of the initial powder is due to the increase in free space between particles and by reducing the area of contact. Thus, the heat transfer from particle to particle, due to the thermal conductivity mechanism, is reduced. This is clearly seen with the combustion of granulated chromium powder. Comparison of the adiabatic burning temperature $T_{ad}$ with

the obtained experimental data showed that the actual burning temperature is higher than the calculated one $T_{ad}$ ($T_{ad}$ = 1280 °C for $Cr_2N$ and $T_{ad}$ = 2060 °C for CrN), with stoichiometric nitrogen content (11.8%—$Cr_2N$, 21.21%—CrN). Thus, combustion was carried out in the co-flow reactor in the superadiabatic heating mode. The experimental existence of superadiabatic heating was proven in [27] when a metal chromium powder was combusted under natural filtration conditions in a high-pressure reactor.

3. Increasing the argon content in the mixture allows a change in the limits of specific flow rate, which allows for obtaining a stable combustion without the formation of a liquid phase. Thus, for a mixture of nitrogen with 12.8% and 24% argon, combustion was able to be carried out at a specific flow rate of 40 $cm^3/(s \cdot cm^2)$. However, the lower limit of flow rate also increased and was 12 $cm^3/(s \cdot cm^2)$. We assume that this is due to a decrease in the amount of fuel when diluted with an inert gas. At 12.8% [Ar], an inverse combustion wave was recorded.
   It was found that, during the combustion of chromium powder with a particle size 63–80 μm in a co-flow of nitrogen with an increase in the specific flow rate from 8 $cm^3/(s \cdot cm^2)$ to 12 $cm^3/(s \cdot cm^2)$, the chromium content increased (from 0 to 2.9 wt.%) with a decrease in the $Cr_2N$ content (from 100 to 97.1 wt.%). Thus, at a specific flow rate of 8 $cm^3/(s \cdot cm^2)$ during the combustion of chromium powder in a co-flow nitrogen, the combustion product was represented only by the $Cr_2N$ phase.
   It was found that, during the combustion of chromium powder with a particle size of 63–80 μm in a co-flow of a nitrogen–argon mixture (argon content 24 wt.%), with an increase in the specific flow rate from 12 to 20 $cm^3/(s \cdot cm^2)$, there was an increase in the chromium content (from 24.8 to 26.7 wt.%) and a decrease in the $Cr_2N$ content (from 75.2 to 73.3 wt.%). Thus, the argon content in the mixture, as well as the value of the specific flow rate, affects the composition of the combustion products.
   Stoichiometric nitrogen content in the chromium mononitride is 21.2% and in the nitride $Cr_2N$ is −11.8%. According to elemental analysis, the samples obtained contain only about 6% to 9.8% $N_2$. Combustion occurs in the mode of incomplete transformation. At the same time, all nitrogen entering the reaction zone fully interacts with chromium. This is supported by data from flow rate sensors at the inlet and outlet of the reactor. In obtained SHS products, as a result of the combustion of both powder and granules of chromium, a slight decrease in nitridation is observed with an increase in the flow rate of the gas mixture (Table 3). Thus, the nitridation of products during the combustion of chromium powder decreased from 8.4% to 8.0% and from 9.5% to 8.7% during the combustion of granular chromium. We assumed that the reason for the decrease in nitridation is the following factor. At the forced filtration mode using a nitrogen–argon mixture, in contrast to natural filtration, there is no "post-nitridation" stage. The reaction cannot continue due to the rapid cooling of the synthesis products by the co-flow of the initial cold gas. Thus, there is a so-called quenching mode. This quenching of burnt materials records the composition of products formed in the high-temperature region.
4. Phase analysis has confirmed the existence of the $Cr_2N$ phase. According to XRD pattern phases (Figure 6), chromium and $Cr_2N$ were detected. Information about the region of existence of the $Cr_2N$ phase is quite contradictory [28,29]. In [29], the homogeneity range is represented in the range of 9.2–11.9% $N_2$. In this paper we obtained the samples with nitrogen containing from 6% to 9.8%. Forced filtration mode allows for the synthesis of non-stoichiometric chromium nitride, $Cr_2N$, of various compositions.
   Studies of the microstructure of synthesized chromium nitride samples showed that the samples obtained in the co-flow filtration mode retained high porosity, and the particles retained their initial cut. The result can be explained by the fact that the maximum temperature in the combustion zone (1640 °C) is significantly lower than the melting temperature in the Cr-N system. The images (Figure 8) show that the microstructure of the particles obtained in the forced filtration mode is single-phase, while the particles after combustion in the natural filtration mode are clearly

two-phase. The lighter areas in the middle of the particles are the $Cr_2N$ phase, and the darker ones are CrN.

## 5. Conclusions

The presented original apparatus allows us to study the combustion process of powder systems in a nitrogen-containing gas mixture in the co-flow filtration mode with a wide range of changes in the initial parameters.

Experimental studies of the combustion of chromium in the co-flow filtration mode have shown the principal possibility of obtaining the non-stoichiometric $Cr_2N$ of different composition. Elemental analysis showed that the nitrogen content in the synthesized $Cr_2N$ samples was in the range of 6.0–9.8%, depending on the characteristics of the initial powder and the operating parameters. It was also found that nitridation tends to decrease with an increase in the specific flow rate of the gas mixture at the reactor inlet. The gas mixture rapidly cools the combustion products, and the synthesis products do not contain chromium mononitride CrN, which is formed under natural filtration conditions in a high-pressure reactor. As the percentage of argon in the nitrogen–argon mixture increases, and the size of the initial chromium powder increases, the temperature and burning rate decrease. The use of forced filtration makes it possible to extend the implementation of SHS in the Cr-$N_2$ system to the area of lower pressures and larger metal particle sizes.

**Author Contributions:** Writing—original draft preparation, N.E.; writing—review and editing, M.Z.; experimental data processing, N.E. and A.T.; methodology, V.R.; formal analysis, Y.R.; supervision, M.Z. and A.Z. All authors have read and agreed to the published version of the manuscript.

**Funding:** The reported study was funded by RFBR, project number 19-38-60036.

**Conflicts of Interest:** The authors declare no conflict of interest.

## References

1. Mukas'yan, A.S.; Martynenko, V.M.; Merzhanov, A.G.; Borovinskaya, I.P.; Blinov, M.Y. Mechanism and principles of silicon combustion in nitrogen. *Combust. Explos. Shock Waves* **1986**, *22*, 534–540. [CrossRef]
2. Sharivker, S.Y.; Borovinskaya, I.P.; Mukas'yan, A.S.; Karpov, V.V. Mechanical activation of powders of silicon and aluminum nitrides produced by the method of self-propagating high-temperature synthesis. *Powder Metall. Met. Ceram.* **1993**, *32*, 189–193. [CrossRef]
3. Sharivker, S.Y.; Borovinskaya, I.P.; Vishnyakova, G.A.; Barinov, Y.N.; Mukas'yan, A.S.; Knyazik, A.M. Morphological and technological characteristics of silicon nitride powder prepared by self-propagating high-temperature synthesis. *Sov. Powder Metall. Met. Ceram.* **1992**, *31*, 915–920.
4. Mukas'yan, A.S.; Stepanov, B.V.; Gal'chenko, Y.A.; Borovinskaya, I.P. Mechanism of structure formation of silicon nitride with combustion of silicon in nitrogen. *Combust. Explos. Shock Waves* **1990**, *26*, 39–45. [CrossRef]
5. Zakorzhevskii, V.V.; Kovalev, I.D.; Barinov, Y.N. Self-propagating high-temperature synthesis of titanium nitride with the participation of ammonium chloride. *Inorg. Mater.* **2017**, *53*, 278–286. [CrossRef]
6. Sytschev, A.E.; Merzhanov, A.G. Self-propagating high-temperature synthesis of nanomaterials. *Russ. Chem. Rev.* **2004**, *73*, 147–159. [CrossRef]
7. Titova, Y.V.; Shiganova, L.A.; Maidan, D.A.; Bichurov, G.V. Self-propagating high-temperature synthesis of nanostructured aluminum nitride powder with the use of aluminum fluoride and sodium azide. *Russ. J. Non-Ferr. Met.* **2014**, *55*, 177–181. [CrossRef]
8. Shoji, Y.; Yoshinaka, M.; Hirota, K.; Yamaguchi, O. Fabrication of bulk chromium nitrides using self-propagating high-temperature synthesis and hot isostatic pressing. *J. Jpn. Soc. Powder Powder Metall.* **2002**, *49*, 323–326. [CrossRef]
9. Hirota, K.; Takano, Y.; Yoshinaka, M.; Yamaguchi, O. Hot Isostatic pressing of chromium nitrides ($Cr_2N$ and CrN) prepared by self-propagating high-temperature synthesis. *J. Am. Ceram. Soc.* **2001**, *84*, 2120–2122. [CrossRef]

10. Yeh, C.L.; Liu, E.W. Combustion synthesis of chromium nitrides by SHS of Cr powder compacts under nitrogen pressures. *J. Alloys Compd.* **2006**, *426*, 131–135. [CrossRef]
11. Aldushin, A.P.; Seplyarskii, B.S.; Shkadinskii, K.G. Theory of filtrational combustion. *Combust. Explos. Shock Waves* **1980**, *16*, 33–40. [CrossRef]
12. Aldushin, A.P.; Merzhanov, A.G.; Seplyarskii, B.S. Theory of filtration combustion of metals. *Combust. Explos. Shock Waves* **1976**, *12*, 285–294. [CrossRef]
13. Aldushin, A.P.; Ivleva, T.P. Coflow filtration combustion in a slit-like reactor: Simultaneous manifestation of fluid-dynamic and thermal instability. *Int. J. Self Propag. High Temp. Synth.* **2014**, *23*, 125–132. [CrossRef]
14. Aldushin, A.P. New results in the theory of filtration combustion. *Combust. Flame* **1993**, *94*, 308–320. [CrossRef]
15. Aldushin, A.P.; Ivleva, T.P. Hydrodynamic instability of the coflow filtration combustion: Numerical simulation. *Dokl. Phys. Chem.* **2013**, *451*, 157–160. [CrossRef]
16. Aldushin, A.P.; Ivleva, T.P. Continuous infiltration-mediated SHS process in a coflow reactor: Numerical modeling. *Int. J. Self Propag. High Temp. Synth.* **2013**, *22*, 77–83. [CrossRef]
17. Babkin, V.S.; Drobyshevich, V.I.; Laevskii, Y.M.; Potytnyakov, S.I. Filtration combustion of gases. *Combust. Explos. Shock Waves* **1983**, *19*, 147–155. [CrossRef]
18. Seplyarskii, B.S.; Vadchenko, S.G.; Kostin, S.V.; Brauer, G.B. Combustion of Ti+0.5C and Ti+C mixtures of bulk density in inert gas coflow. *Combust. Explos. Shock Waves* **2009**, *45*, 30–37. [CrossRef]
19. Seplyarskii, B.S.; Brauer, G.B.; Tarasov, A.G. Combustion of the gasless system Ti + 0.5C in a nitrogen coflow. *Combust. Explos. Shock Waves* **2011**, *47*, 294–301. [CrossRef]
20. Seplyarskii, B.S.; Kostin, S.V.; Brauer, G.B. Dynamic combustion regimes of the Ti-(Ti+0.5C) layered system in a concurrent nitrogen flow. *Combust. Explos. Shock Waves* **2008**, *44*, 655–661. [CrossRef]
21. Seplyarskii, B.S.; Kochetkov, R.A.; Lisina, T.G. Convective Combustion of a Ti + 0.5C Granulated Mixture. Domain of Existence and Fundamental Phenomena. *Combust. Explos. Shock Waves* **2019**, *55*, 295–299. [CrossRef]
22. Seplyarskii, B.S.; Kochetkov, R.A. A Study of the Characteristics of the Combustion of Ti + xC (x > 0.5) Powder and Granular Compositions in a Gas Coflow. *Russ. J. Phys. Chem. B* **2017**, *11*, 798–807. [CrossRef]
23. Salgansky, E.A.; Kislov, V.M.; Glazov, S.V.; Zholudev, A.F.; Manelis, G.B. Filtration combustion of a carbon-inert material system in the regime with superadiabatic heating. *Combust. Explos. Shock Waves* **2008**, *44*, 273–280. [CrossRef]
24. Salgansky, E.A.; Kislov, V.M.; Glazov, S.V.; Zholudev, A.F.; Manelis, G.B. Specific features of filtration combustion of a pyrolized solid fuel. *Combust. Explos. Shock Waves* **2010**, *46*, 528–532. [CrossRef]
25. Glazov, S.V.; Salganskii, E.A.; Kislov, V.M.; Salganskaya, M.V.; Zholudev, A.F. Change in the structure of the filtration combustion wave due to a fuel composition change. *Combust. Explos. Shock Waves* **2010**, *46*, 286–292. [CrossRef]
26. Braverman, B.; Ziatdinov, M.; Maksimov, Y. Chromium combustion in nitrogen. *Combust. Explos. Shock Waves* **1999**, *35*, 501–505. [CrossRef]
27. Braverman, B.; Ziatdinov, M.; Maksimov, Y. Superadiabatic heating in combustion chromium in nitrogen. *Combust. Explos. Shock Waves* **1999**, *35*, 645–647. [CrossRef]
28. Mills, T. The thermodinamic relations in the chromium-nitrogen system. *J. Less-Common Met.* **1972**, *26*, 223–234. [CrossRef]
29. Lyakishev, N.P. (Ed.) *State Diagrams of Double Metal Systems: A Reference Book*; Mashinostroyeniye: Moscow, Russia, 1997; Volume 2, pp. 142–144.




© 2020 by the authors. Licensee MDPI, Basel, Switzerland. This article is an open access article distributed under the terms and conditions of the Creative Commons Attribution (CC BY) license (http://creativecommons.org/licenses/by/4.0/).